Molecular Biology of the Cell
Vol. 6, 525–539, May 1995

Novel PI(4)P 5-Kinase Homologue, Fab1p, Essential for Normal Vacuole Function and Morphology in Yeast

Ayumu Yamamoto,* Daryll B. DeWald,† Igor V. Boronenkov,‡ Richard A. Anderson,‡ Scott D. Emr,† and Douglas Koshland*§

*Carnegie Institution of Washington, Department of Embryology, Baltimore, Maryland 21210; †Division of Cellular and Molecular Medicine & The Howard Hughes Medical Institute, University of California, San Diego, School of Medicine, La Jolla, California 92093-0668; and ‡Department of Pharmacology, University of Wisconsin Medical School, Madison, Wisconsin 53706

Submitted January 31, 1995; Accepted March 13, 1995
Monitoring Editor: Randy W. Schekman

The *FAB1* gene of budding yeast is predicted to encode a protein of 257 kDa that exhibits significant sequence homology to a human type II PI(4)P 5-kinase (PIP5K-II). The recently cloned human PIP5K-II specifically converts PI(4)P to PI(4, 5)P_2 (Boronenkov and Anderson, 1995). The region of highest similarity between Fab1p and PIP5K-II includes a predicted nucleotide binding motif, which is likely to correspond to the catalytic domain of the protein. Interestingly, neither PIP5K-II nor Fab1p exhibit significant homology with cloned PI 3-kinases or PI 4-kinases. *fab1* mutations result in the formation of aploid and binucleate cells (hence the name *FAB*). In addition, loss of Fab1p function causes defects in vacuole function and morphology, cell surface integrity, and cell growth. Experiments with a temperature conditional *fab1* mutant revealed that their vacuoles rapidly (within 30 min) enlarge to more than double the size upon shifting cells to the nonpermissive temperature. Additional experiments with the *fab1 ts* mutant together with results obtained with *fab1 vps* (vacuolar protein sorting defective) double mutants indicate that the nuclear division and cell surface integrity defects observed in *fab1* mutants are secondary to the vacuole morphology defects. Based on these data, we propose that Fab1p is a PI(4)P 5-kinase and that the product of the Fab1p reaction, PIP_2, functions as an important regulator of vacuole homeostasis perhaps by controlling membrane flux to and/or from the vacuole. Furthermore, a comparison of the phenotypes of *fab1* mutants and other yeast mutants affecting PI metabolism suggests that phosphoinositides may serve as general regulators of several different membrane trafficking pathways.

INTRODUCTION

Phosphatidylinositol 4,5-bisphosphate (PIP_2) is a minor, highly acidic phospholipid that is synthesized by two successive phosphorylations of phosphatidylinositol (PI). First, PI is phosphorylated by PI 4-kinase to generate PI(4)P, and then PI(4)P is phosphorylated by PI(4)P 5-kinase to generate PIP_2. The biosynthesis of PIP_2 has attracted increasing interest because of mounting evidence implicating metabolites of PIP_2 as important regulators of many cellular processes. For example, the breakdown of PIP_2 by phospholipase C (PLC) generates diacylglycerol and inositol 1,4,5-triphosphate (IP3) (Berridge and Irvine, 1989). Diacylglycerol activates protein serine/threonine kinase C (PKC) while IP3 stimulates the release of Ca^{2+} from intracellular storage sites. The activated kinase and the rise in intracellular calcium are thought to play an important role both in mediating signal transduction from the cell surface to the nucleus and in regulating nuclear events. PIP_2 also can be further phosphorylated by PI 3-kinase to generate phosphatidylinositol 3,4,5-trisphosphate (PIP_3) (Kapeller and Cantley, 1994). PIP_3 has been implicated in stimulating kinases

§ Corresponding author.

Table 1. Genotypes of strains

Strain	Genotype	Source
801-6-1	*Mata bar1 ade3 trp1 gal1*	This study
4506-9-4	*Mata his3 leu2 ura3 gal1*	This study
5317-2-2	*Matα leu2 gal1*	This study
616-3-2	*Mata fab1-1 ade3 trp1 can1 cyh1 gal1*	This study
672-5-2	*Mata fab1-2 his3 leu2 ura3 gal1*	This study
663D-1-3	*Matα fab1-Δ1 his7 leu2 ura3 gal1*	This study
660-6-1	*Matα fab1-2 leu2 ura1 can1 cyh2 gal1*	This study
6742-1-1	*Mata his3 leu2 lys2 trp1 ura3 suc2*	This study
6742-1-2	*Matα fab1::LEU2 vps18::TRP1 his3 leu2 lys2 trp1 ura3 suc2*	This study
6742-1-3	*Matα fab1::LEU2 ade2 his3 leu2 trp1 ura3 suc2*	This study
6742-1-4	*Mata vps18::TRP1 ade2 his3 leu2 trp1 ura3 suc2*	This study
JSR18Δ1	*Matα vps18::TRP1 his3 leu2 lys2 trp1 ura3 suc2*	Emr lab.
5309-100	*Matα vps5::HIS3 his3 leu2 lys2 trp1 ura3 suc2*	Emr lab.
5313-100	*Matα vps19-1 his3 leu2 lys2 trp1 ura3 suc2*	Emr lab.
5312-100	*Matα vps33::HIS3 his3 leu2 lys2 trp1 ura3 suc2*	Emr lab.
PHY102	*Matα vps34::TRP1 his3 leu2 lys2 trp1 ura3 suc2*	Emr lab.
SY2623	*Matα ste3::URA3 GAL-STE3(myc tagged) ren1-1 ade1 ade2 his6 leu2 met14 trp1 ura3 pep4Δ*	Nick Davis
7031	*Matα fab1::LEU2 vps18::TRP1 his3 leu2 lys2 trp1 ura3 suc2*	This study
6752-1-3	*Matα fab1::LEU2 vps5::HIS3 his3 leu2 lys2 trp1 ura3 suc2*	This study
6772-1-3	*Matα fab1::LEU2 vps33::HIS3 his3 leu2 lys2 trp1 ura3 suc2*	This study
FV19-1	*Matα fab1::LEU2 vps19-1 his3 leu2 lys2 trp1 ura3 suc2*	This study
FV34-1	*Matα fab1::LEU2 vps34::TRP1 his3 leu2 lys2 trp1 ura3 suc2*	This study
AY2623-1	*Matα fab1::LEU2 ste3::URA3 GAL-STE3(myc tagged) ren1-1 ade1 ade2 his6 leu2 met14 trp1 ura3 pep4Δ*	This study

necessary for mitogenic activation, and possibly modulating actin assembly (Lassing and Lindberg, 1988; Janmey and Stossel, 1989; Kapeller and Cantley, 1994). Finally, recent evidence indicates that PIP_2 itself may have important regulatory roles as it binds to several actin-associated proteins and acts as a co-factor for phospholipase D (Janmey, 1994; Liscovitch *et al.*, 1994).

Recent efforts have focused on the identification and characterization of the enzymes involved in PIP_2 metabolism. PI 3-kinases, PI 4-kinases, and PI(4)P 5-kinases as well as PLC have now been identified biochemically in many organisms (Bazenet *et al.*, 1990; Carpenter and Cantley, 1990; Ling *et al.*, 1990; Buxeda *et al.*, 1991; Flanagan and Thorner, 1992; Kapeller and Cantley, 1994). With such enzymes in hand, it is possible to isolate the genes that encode them, and to use genetics to begin to assess their function in vivo.

This strategy has been most successfully employed in the yeast *Saccharomyces cerevisiae*. Two different PI 4-kinases have been identified in yeast. One is essential for growth (Pik1p) whereas inactivation of the other PI 4-kinase (Stt4p) results in osmosensitivity similar to that seen in yeast PKC mutants (Flanagan *et al.*, 1993; Yoshida *et al.*, 1994a). Osmosensitivity has also been observed in yeast mutants defective for PLC activity but these mutants also are impaired in some nutritional responses and in chromosome transmission (Flick and Thorner, 1993; Payne and Fitzgerald-Hayes, 1993). Mutants defective in a PI 3-kinase (Vps34p) exhibit a severe defect in protein sorting to the yeast vacuole/lysosome but not to the cell surface (Herman and Emr, 1990; Schu *et al.*, 1993). These results suggest that the product of Vps34p activity, PI(3)P, may serve as a specific regulator of vesicle-mediated protein traffic from the Golgi to the vacuole (Herman *et al.*, 1992). In summary, the diverse phenotypes of yeast mutants defective in PI metabolism suggest that phosphoinositides function as regulators of many aspects of cell physiology.

Although rapid progress in understanding PIP_2 synthesis and function is being made, an important missing link in this endeavor is the identification and characterization of PI(4)P 5-kinases. In this report, we identify a yeast gene *FAB1* (formation of aploid and binucleates) that contains extensive similarity to a human PI(4)P 5-kinase. This gene was identified initially because *fab1* mutations caused aberrant chromosome segregation in budding yeast. Further analysis showed that *fab1* mutants had additional defects in cell surface integrity and in vacuole morphology and function. The mechanism by which the Fab1 protein affects multiple cellular processes is discussed in the context of its putative PI(4)P 5-kinase activity.

MATERIALS AND METHODS

Yeast Strains and Media

Yeast strains and genotypes are shown in Table 1. YPD medium contained 1% yeast extract, 2% peptone, and 2% glucose. Synthetic medium was described previously (Rose *et al.*, 1990).

Reagents

4',6'-Diamidino-2-phenylindole (DAPI) and quinacrine were purchased from Sigma Chemical (St. Louis, MO). 6-Carboxyfluorescein diacetate (6-CFDA), and 5-(and 6-)carboxy-2',7'-dichlorofluorescein diacetate (CDCFDA) were purchased from Molecular Probes (Eugene, OR).

Isolation of Mutants

Wild-type strain 801–6-1 was mutagenized by ethylmethane sulfonate to 50% viability. The mutagenized cells were spread on YPD plates and tested for growth at 23°C and 37°C. About 800 mutants, which grew at 23°C but not at 37°C, were isolated. The *ts* lethal mutants were grown in YPD medium at 23°C to log phase and shifted to 37°C. After a 4-h incubation at 37°C, cells were fixed by adding 1/10 vol of 37% formaldehyde to the culture. Fixed cells were washed with water and stained with DAPI at 100 ng/ml. Abnormal nuclear segregation was analyzed using a Zeiss Axiophot microscope equipped with epifluorescent and Nomarski optics. Isolated mutants that showed abnormal nuclear segregation were backcrossed five or six times to strains congenic to 801–6-1 to clean up the genetic background.

Labeling of Vacuoles with Fluorescent Dyes

Cells were labeled with quinacrine or 6-CFDA as described by Preston *et al.* (1992). Cells in log phase were incubated at 37°C for 4 h and harvested. Cells were resuspended in YPD medium containing 5 μM 6-CFDA and 50 mM citric acid (pH 3.0) and incubated at 37°C for 30 min. The labeled cells were cooled down to 0°C on ice and resuspended in YPD medium at 0°C. 6-CFDA–labeled cells were analyzed under a microscope or by flow cytometry within 2 h after labeling (see below). Vacuoles were stained with CDCFDA as described previously (Roberts *et al.*, 1991).

Flow Cytometric Analysis

For the analysis of DNA content, cells were fixed with 70% ethanol and stained with propidium iodide as described (Hutter and Eipel, 1978). The DNA content of 25,000 cells in each sample were determined with a Coulter EPICS 752 flow cytometer. For pH analysis of vacuoles, cells were labeled with 6-CFDA as described above. The fluorescence ratio between two emissions obtained by excitations at 458 nm and 488 nm was analyzed.

Indirect Immunofluorescence

Cells were processed for indirect immunofluorescent microscopy as described (Kilmartin and Adams, 1984). Microtubules were detected by rat monoclonal anti-α-tubulin antibody YOL1/34 (Kilmartin *et al.*, 1982) diluted 1–200 and rhodamine-conjugated goat anti-mouse antibody (Cappel Labs., Cochranville, PA) diluted 1–200 in solution F (0.1% bovine serum albumin, 0.1% sodium azide, 0.85% sodium chloride, and 10 mM potassium phosphate, pH 7.4

Spotting Assay

Cultures containing different plasmids were grown in selective medium to log phase at 23°C. Cultures at 7×10^6 cells/ml were serially diluted to generate cell cultures whose cell densities differed by fivefold. Five microliters of each diluted cell suspension was spotted on the selective solid medium and the plate was incubated at 23°C or 37°C for several days.

Cloning, Mapping, Sequence Analysis, and Plasmid Construction of FAB1 gene

The *FAB1* gene was cloned by complementation of the recessive *ts* lethality associated with the *fab1–1* allele. 616–3-2 cells carrying the *fab1–1* mutation were transformed (Ito *et al.*, 1983) with a yeast genomic library constructed in the centromere-based plasmid pRS200 (Connelly and Hieter, unpublished data). Approximately 3000 transformants were replica plated onto YPD plates and tested for growth at 37°C. The plasmids containing identical ~9-kb inserts of yeast DNA were isolated from nine transformants that grew at 37°C. One of the plasmids, p6161–8-3, was processed for further use. The DNA insert cut out from p6161–8-3 by *Sal*I and *Bgl*II was recloned into pRS314 and the resultant plasmid was designated as pAY11. A 6-kb *Pst*I fragment of p6161–8-3, which was the shortest DNA fragment retaining the complementation activity (see Figure 6), was subcloned into the *Pst*I site of pRS314. Plasmids containing the *Pst*I fragment in the same or opposite direction to pAY11 were designated as pAY36 or pAY33, respectively.

To verify that the insert contained the authentic *FAB1* gene, the ~9-kb insert was cut out by *Eag*I and *Sal*I, and recloned into a plasmid, pRS304, which contains *ARS* and *TRP1* but not a yeast centromere. This plasmid, designated as pAY3, was cut at a *Bam*HI site in the insert and transformed into a *trp1* wild-type strain 618–4-2. The *FAB1* gene was mapped by using a chromo blot and a cosmid clone grid filter (gift of Linda Riles, University of Washington, St. Louis) probed by the 6-kb *Pst*I fragment of the 9-kb DNA insert.

For sequencing, a nested set of deletions of pAY11 and pAY33 was generated by digesting with *Exo*III from the *Eco*RI site. The DNA sequence of one strand of pAY11 and pAY33 were determined as described by Applied Biosystems (Foster City, CA). Gaps between the DNA sequences were filled by additional sequencing utilizing 18-base primers complementary to the sequence adjacent to the gaps. The DNA sequence of the N-terminus of *FAB1* gene was obtained by sequencing both strands of a *Hin*dIII fragment of a lambda phage clone I-1B12 (Yoshikawa and Isono, 1991). A homology search was carried out by using a TBLASTN program.

The fragment excised from pAY33 by *Hin*dIII and *Eco*RI was recloned between *Hin*dIII and *Eco*RI sites of pRS416 (pAY59). The *Hin*dIII fragment of I-1B12 was inserted at the *Hin*dIII site of pAY59. The resultant plasmid was designated as pAY60; it contained the whole open reading frame of the *FAB1* gene. A partial *FAB1* gene, which was originally cloned and lacked the N terminus, was cut out from pAY36 by *Sal*I and *Eag*I and recloned between *Xho*I and *Sal*I of pRS416 to generate pAY64. pAY60 and pAY64 were tested for their ability to complement the *fab1–2 ts* lethality by a spotting assay.

Construction of ΔFAB1 Strains

To delete the C-terminal region of Fab1p (Figure 7C, *fab1::LEU2*), a *Bgl*II fragment encoding the *LEU2* gene was inserted at the *Bam*HI site of the *FAB1* open reading frame on the p6161–8-3 plasmid. A *Pst*I-*Sph*I fragment of the *FAB1* gene containing the *LEU2* insertion plasmid was ligated between the *Pst*I and *Sph*I sites of a bacterial plasmid pUC19. The resultant plasmid pAY10 was digested with *Pst*I and *Mlu*I, and transformed (Ito *et al.*, 1983) into *leu2* strains. To delete almost the entire region of the *FAB1* open reading frame (Figure 7C, *fab1-Δ1*), a *Sal*I-*Sma*I fragment encoding the *LEU2* gene was inserted between one of the *Sal*I sites closer to the N-terminus and the *Nru*I site of the *FAB1* open reading frame on pAY60. An *Apa*I-*Pst*I fragment of the *FAB1* gene containing the *LEU2* insertion was purified and transformed into *leu2* strains. Deletions of the genomic *FAB1* gene in *leu*$^+$ transformants were confirmed by Southern blot analysis (Rose *et al.*, 1990).

Cell Labeling and Immunoprecipitation

For analysis of CPY processing, whole yeast cells were labeled essentially as described (Herman and Emr, 1990). Cells were pulse-labeled with Expre^{35}S-label (NEN Radiochemicals, Boston, MA) for 15 min at either 23°C (Δ*fab*) or 37°C (SEY6210 and *fab1–2*) and chased at the same temperatures for the indicated times by the addition of methionine and cysteine to 5 mM and 1 mM, respec-

tively. After the chase, the proteins were precipitated by the addition of trichloroacetic acid to a final concentration of 6%. Immunoprecipitation of CPY was performed as described previously (Herman and Emr, 1990) and samples were electrophoresed on 10% sodium dodecyl sulfate-polyacrylamide gels. After electrophoresis, gels were fixed in 40% methanol/10% acetic acid, washed twice with water, incubated in 1.0 M sodium salicylate/1% glycerol, then dried and subjected to autoradiography.

Vacuole Size Measurement

The *fab1–2* ts strain was grown to mid-log phase at 23°C and shifted to 37°C for the indicated times. Vacuole measurements were taken from photographs of cells affixed to glass slides (using Nomarski optics) or from images generated by electron microscopy.

RESULTS

Isolation of fab Mutants

When the orientation of the mitotic spindle is defective in *S. cerevisiae*, both sets of replicated chromosomes are inherited by either the mother or the bud (Palmer *et al.*, 1990). This aberrant event leads to the formation of aploid and binucleate cells (*fab* phenotype). To isolate *fab* mutants, we made a collection of 742 mutants that were temperature sensitive (*ts*) for growth. Cultures of these mutants were exposed to the restrictive temperature (37°C) for 4 h, fixed, stained with a DNA-specific dye (DAPI), and then examined under the microscope for the *fab* phenotype. Seven mutants showed a temperature-dependent *fab* phenotype. Both the *ts*-growth and temperature-dependent fab phenotype of these mutants were recessive and cosegregated during multiple backcrosses. In the process of backcrossing these mutants, we discovered two additional *ts* phenotypes of *fab* mutants, enlarged vacuoles and aberrant cell shape. All mutant phenotypes co-segregated with each other and segregated 2:2 from the corresponding wild-type phenotype. Therefore, the mutant phenotypes were caused by a mutation(s) at a single locus. All seven *fab* mutants also failed to complement one another for any of the mutant phenotypes, suggesting that they contained alleles of a common gene. We named this gene *FAB1*. As the phenotypes of the seven *fab1* mutants appeared indistinguishable, most subsequent experiments were carried out with strains bearing *fab1–2*.

Analysis of ts Growth of fab1 Strains

To assess whether the function of the *FAB1* product is essential for growth, we cloned the *FAB1* gene (see MATERIALS AND METHODS) and used it to construct a deletion allele (*fab1-Δ1*) that removed all but 41 of the 2279 residues encoded by the putative *FAB1* ORF (see below). The deletion initially was introduced into a diploid strain. Haploid segregants containing *fab1-Δ1* grew slowly at 23°C and did not grow at 37°C (Figure 1). Similar results were obtained with *fab1::LEU2*, another putative disrupting allele of the *FAB1* gene (see below). These results demonstrated that the *FAB1* gene is important for growth at 23°C and essential at 37°C.

To further assess the consequences of shifting the *fab1–2* mutant to 37°C, the mutant was examined in the light microscope after exposure to the nonpermissive temperature. The mutant cells did not arrest at a specific point in the cell cycle. However, after 4

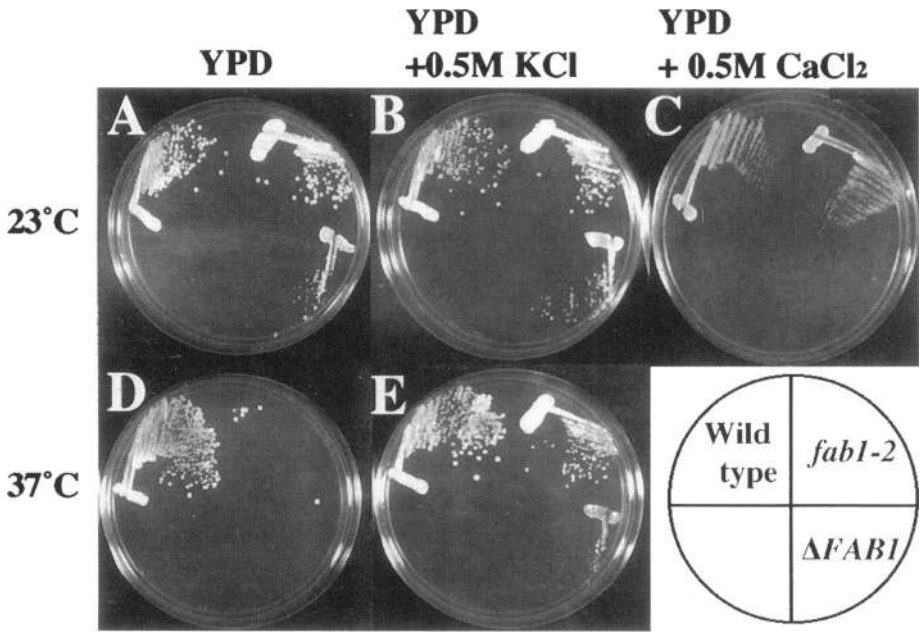

Figure 1. Ts lethality, osmoremediation, and Ca sensitivity of *fab1* mutants. Wild-type (4506–9-4), *fab1–2* (672–5-2), and *fab1-Δ1* (663D-1–3) cells were streaked onto YPD agar plates with or without $CaCl_2$ or KCl as indicated. Plates were incubated at 23°C or 37°C and photographed after colonies were visible.

h at the nonpermissive temperature, ~25% of the *fab* cells had lysed as evidenced by staining with trypan blue. This result suggested that *fab* mutants had a cell surface defect. As the *ts*-lethality of other cell lysis mutants can be suppressed by changes in osmolarity (Yoshida *et al.*, 1994a), we compared the ability of *fab1* and wild-type cells to form colonies on solid medium supplemented with different osmotic supports. The presence of 0.5 M KCl (Figure 1) or 1 M sorbitol (Yamamoto and Koshland, unpublished results) in the growth medium significantly suppressed the ts-growth defect of the *fab1–2* mutant and partially suppressed the ts-growth defect of the *fab1-Δ1* mutant. In contrast, 0.5 M $CaCl_2$ inhibited the growth of the *fab1-Δ1* strain but not the *fab1–2* or *FAB1* strains (Figure 1). Therefore, *fab1* mutants appeared osmoremedial and Ca-sensitive.

fab1 Mutants Accumulate very large Vacuoles

Vacuole morphology in *fab1* mutants and wild-type cells was characterized using a vacuole-specific vital dye CDCFDA (Roberts *et al.*, 1991). When wild-type cells were grown at 23°C, vacuoles appeared as several small organelles that occupied a small fraction of the total cell vol (Figure 2). At 37°C the number of vacuoles decreased while their size increased slightly. In contrast, when *fab1–2* cells were grown at 23°C, vacuoles were already larger than vacuoles in wild-type cells at 37°C. In addition, when a *fab1–2* culture was grown at 37°C for 4 h, >90% of the cells contained a single large vacuole. The vacuole morphology in *fab1-Δ1* and *fab1::LEU2* cells was similar to *fab1–2* cells except that large vacuoles were already present at 23°C in the *fab1-Δ1* and *fab1::LEU2* cells. Hence, *fab1* mutations result in a vacuole morphology defect.

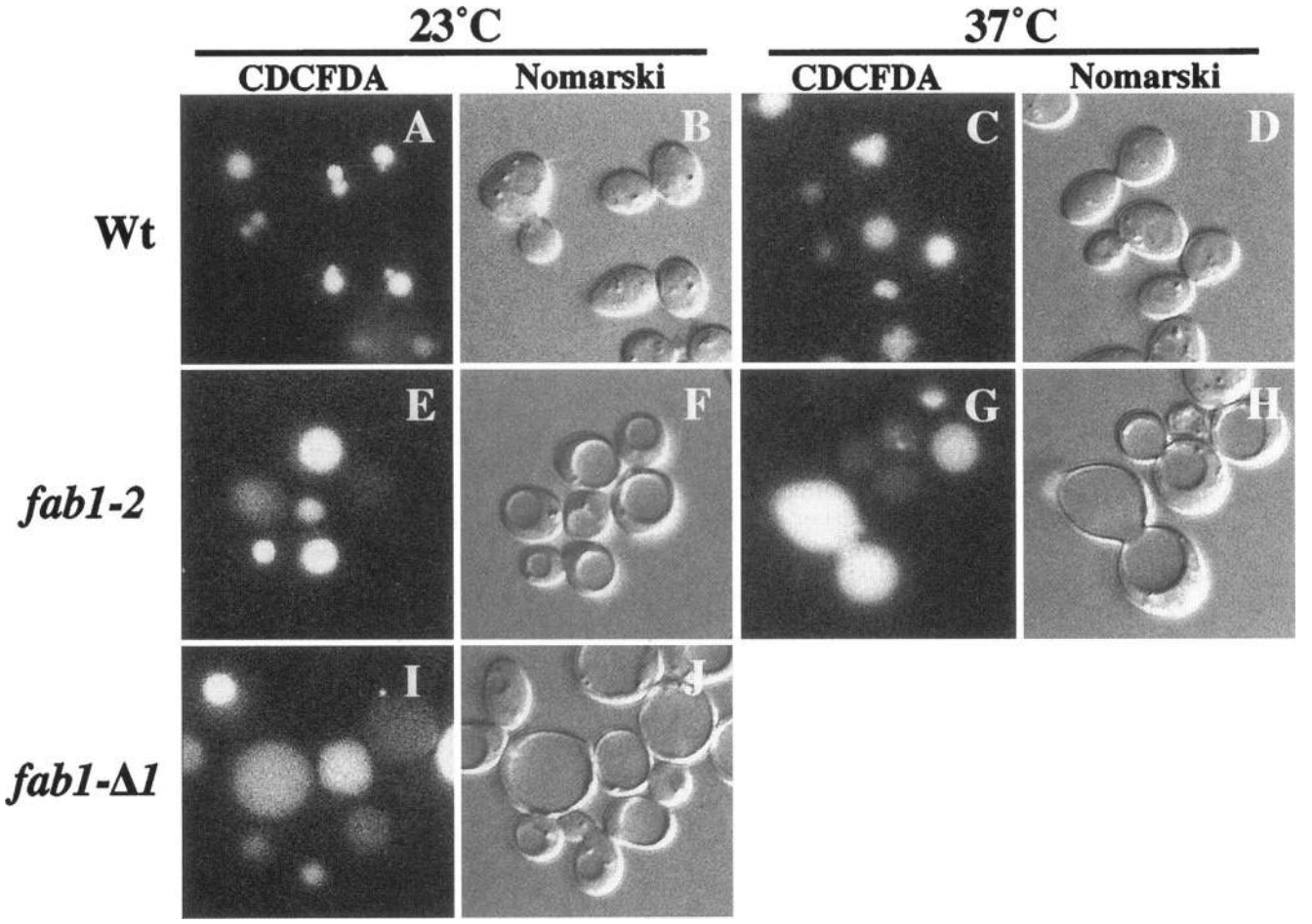

Figure 2. Vacuoles visualized by CDCFDA staining and Nomarski optics. Wild-type cells (4506–9-4; A, B, C, and D), *fab1–2* mutant cells (672–5-2; E, F, G, and H), and *fab1-Δ1* cells (663D-1–3; I and J), were grown to log phase at 23°C (A, B, E, F, I, and J) and incubated at 37°C for 4 h (C, D, G, and H). Cells were stained with CDCFDA and vacuolar morphology was analyzed (see MATERIALS AND METHODS).

In *fab1* cells, the vacuole was visible by Nomarski optics (compare Nomarski and CDCFDA images in Figure 2) allowing us to use Nomarski images (N>100) to quantitate vacuole size. When *fab1–2* cells were grown at 23°C, the average diameter of the vacuole was 1.6 μm (± 0.4). When these cells were grown at 37°C for 30 min, the average diameter increased to 2.4 μm (± 0.5), and then remained constant for at least 2 h. No significant change in average diameter of the cell was observed over the same time course. Similar results were obtained when vacuole diameter was followed in electron micrographs (data not shown). This difference in the average diameter predicts a 250% increase in the average vacuole surface area. Therefore, upon temperature shift, the enlargement of the vacuole in *fab1–2* cells is both significant and rapid.

Abnormal vacuole morphology is also a phenotype of some vacuole protein sorting (*vps*) mutants (Klionsky *et al.*, 1990). These mutants missort and secrete precursor forms of soluble vacuolar hydrolases like carboxypeptidase Y (CPY). Because CPY undergoes a series of compartment-specific modifications as it transits the early stages of the secretory pathway, its sorting or missorting is easily scored by following its processing and maturation via pulse-chase immunoprecipitation experiments (Klionsky *et al.*, 1990). To address whether *fab1* mutants had both vacuole morphology and protein sorting defects like *vps* mutants, we examined CPY processing and maturation in *fab1* mutants.

In the experiment shown in Figure 3, wild-type and *fab1–2* cells were grown at 25°C, then preshifted to 37°C for 60 min before labeling. In both cell types the major precursor forms of CPY (p1CPY and p2CPY) and a small amount of mature CPY (mCPY) were found after labeling for 15 min with [^{35}S]methionine/cysteine at 37°C (T = 0, Figure 3). Chase was initiated by addition of excess unlabeled methionine and cysteine. Thirty minutes after the chase was added (T = 30, Figure 3), most of the CPY was fully processed to the mature form, and no CPY was missorted to the cell surface (DeWald and Emr, unpublished results). Therefore, the enlargement of the vacuole, which occurs in *fab1–2* mutants 30 min after shift to the nonpermissive temperature, does not appear to be caused by a defect in the processing or sorting of vacuolar proteins.

In the *fab1::LEU2* strain labeled and chased at 25°C, however, a defect in CPY maturation was observed (Figure 3). Even after 60 min of chase, less than 20% of CPY was converted to the mature form. An aberrantly processed form (*) accumulated distinct from p1CPY and p2CPY. The failure to process CPY properly in *fab1::LEU2* strains indicates that the loss of *FAB1* activity eventually leads to a defect in vacuolar protein maturation. This defect may reflect a problem with

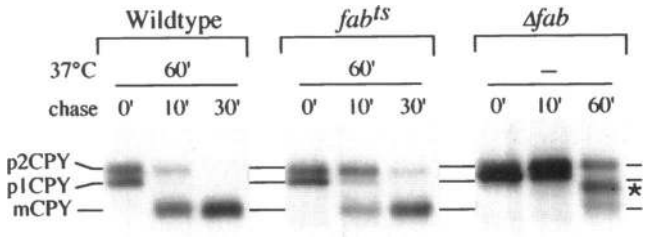

Figure 3. CPY sorting in wild-type and *fab* mutant strains. Intracellular sorting of CPY was assessed in whole cells by preincubating cells at 37°C (wild type and *fab ts* for 60 min) before pulse labeling for 15 min. Cells were then chased with excess unlabeled methionine and cysteine, proteins were precipitated with TCA, and CPY was immunoprecipitated and analyzed by sodium dodecyl sulfate-polyacrylamide gel electrophoresis and autoradiography. p1CPY and p2CPY refer to precursor forms and mCPY corresponds to the mature protein, which has arrived at the vacuole.

CPY maturation in the vacuole or with CPY localization to the vacuole. The *fab1::LEU2* mutants did not secrete CPY (DeWald and Emr, unpublished results); therefore, if CPY is mislocalized in this mutant, it is not secreted as has been observed in the *vps* mutants.

fab1 Mutants Exhibit Defects in Vacuole Function

In the Nomarski images, the refractivity of the vacuole differed between *fab1–2* and wild-type cells both at 23°C and 37°C (Figure 2). This result suggested that *fab1* mutations potentially affected vacuole content and/or function as well as its size. One parameter of vacuole function is its pH, which can be assessed qualitatively using quinacrine, a dye that exhibits pH-dependent staining of the vacuole. When wild-type and *fab1* cells were stained with quinacrine, *fab1–2* vacuoles did not stain as well as wild-type vacuoles at both 23°C and 37°C (data not shown). This observation suggested that the pH of vacuoles in *fab1* mutants was partially affected even at the permissive temperature.

We quantified the pH of vacuoles using the dye 6-CFDA and dual-excitation flow cytometry (Figure 4). Fluorescent ratio profiles were obtained for wild-type and *fab1–2* cells grown at 37°C. To generate standard profiles, wild-type cells were allowed to accumulate the dye in their vacuoles, and then the pH of the vacuole was equilibrated with different buffers containing a proton-pump uncoupler (see MATERIALS AND METHODS). A comparison of these profiles showed that the pH of the wild-type vacuole was around 6.0 whereas the pH of *fab1* vacuoles was 7.0 or higher. The pH for wild-type vacuoles was similar to the previously reported values (Preston *et al.*, 1992). These results demonstrated that *fab1* mutants had defects in acidification of vacuoles.

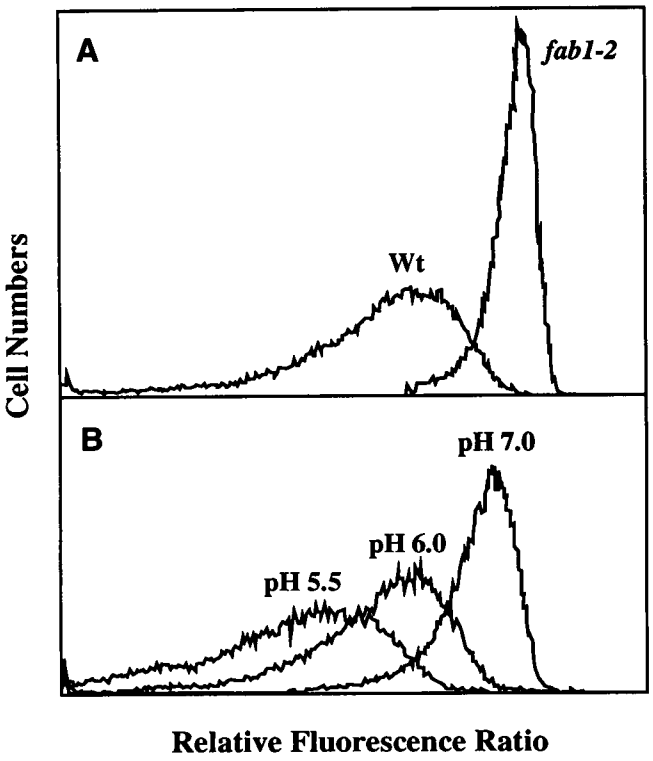

Figure 4. Flow cytometric analysis of the pH of vacuoles. Wild-type cells (4506–9-4) and *fab1*–2 cells (672–5-2) were grown to log phase at 23°C, exposed to 37°C for 3 h, and labeled with 6-CFDA (see MATERIALS AND METHODS). The labeled cells were analyzed by dual-excitation flow cytometry (A). For standards, the labeled wild-type cells were resuspended in different buffers in the presence of proton-pump uncouplers and processed for flow cytometric analysis (B).

fab1 Mutant Shows Abnormal Chromosome Transmission and Spindle Morphology

The formation of aploid and binucleate cells by *fab1* mutants suggested a defect in nuclear division. To examine this phenotype more extensively, the distributions of chromosomes and microtubules were examined in *fab1*–2 mutants and wild-type cells by standard microscopic methods (Table 2 and Figure 5). When *fab1*–2 and wild-type cells were grown at 23°C, no differences in the distribution of chromosomes and microtubules were observed. By 4 h after shift to 37°C, 56% of *fab1*–2 cells exhibited heterogeneous chromosome (Table 2) and microtubule (Figure 5) distributions that were rarely if ever observed in wild-type cells. For example, more than 20% of the cells became aploid and binucleate (Figure 5, C and D, large arrowheads and arrows), which was an increase of at least 100-fold compared with wild-type cells (Palmer *et al.*, 1990; Sullivan and Huffaker, 1992). Even in cells containing only a single nucleus, the positions of the chromosomal mass and spindles were often aberrant (see legend to Figure 5). These results suggested that *fab1* mutants were defective in spindle position and chromosome segregation. Similar results were obtained with cultures of *fab1*-Δ*1* (Table 2) and *fab1::LEU2* (Yamamoto and Koshland, unpublished results) mutants except some cells in these cultures exhibited abnormal chromosome segregation even at 23°C.

Further evidence of abnormal chromosome transmission in *fab1*–2 cells was obtained when the DNA

Table 2. Distribution of cell types in *fab1-2*

Genotype	Temp (°C)	Time (hr)	⊙	⊙	⊙⊙	⊙⊙	⊙⊙	(1)	(2)	(3)	Others
							(%)				
FAB1[a]	23		39	33	29	3	8	0	0	0	0
	37	4	39	28	13	2	9	0	0	0	0
fab1-2[b]	23		34	36	22	2	7	0	0	0	0
	37	2	36	29	13	4	2	0	5	6	9
	37	4	23	15	5	2	2	9	15	16	16
fab1-Δ*1*[c]	23	—	20	30	18	3	4	7	9	5	4

Cells were grown in YPD medium at 23°C to log phase and shifted to 37°C.

Aliquots were fixed, and stained by DAPI at designated times. Cell types of 200 cells were analyzed and shown in percentage.

[a]Strain 4506-0-4

[b]Strain 672-5-2

[c]Strain 663D-1-3

(1) Aploid cells.

(2) Binucleate cells.

(3) Large budded cells containing single nucleus off the bud neck.

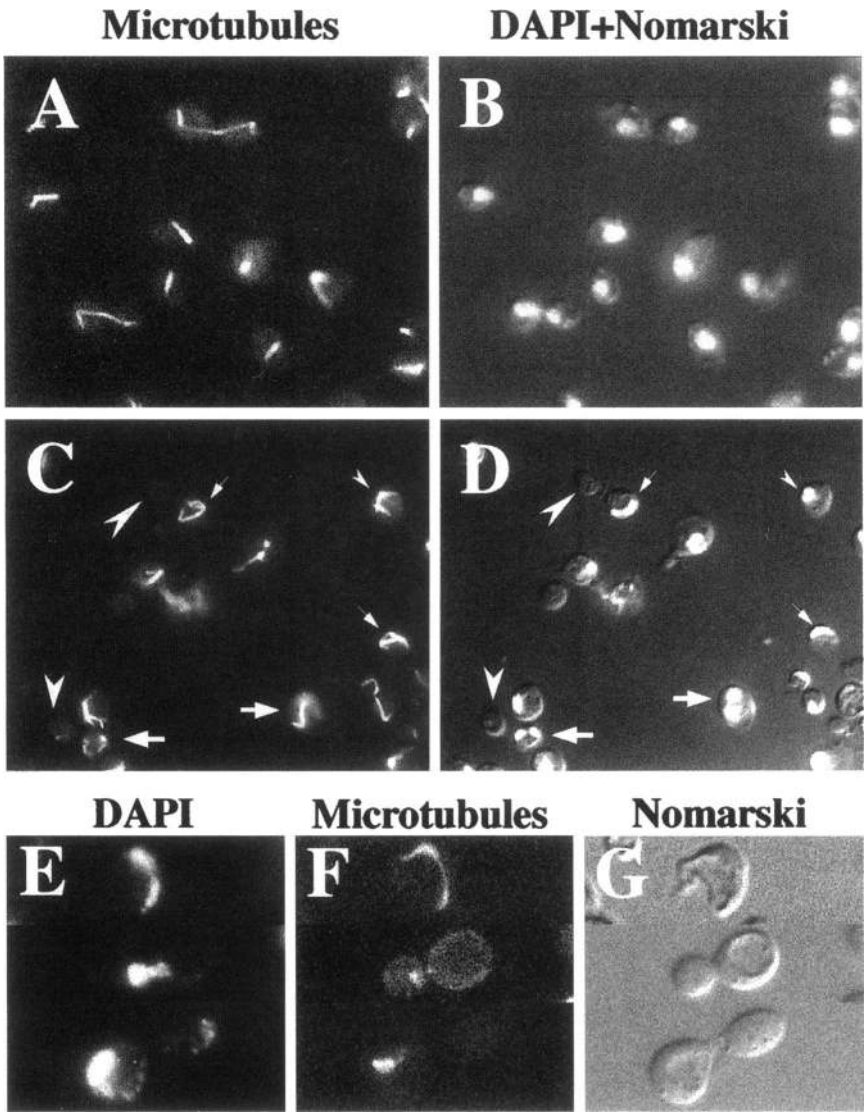

Figure 5. Micrographs showing nuclear and microtubule morphology of *fab1* and wild-type cells. Wild-type (4506–9-4; A and B) and *fab1–2* (660–6-1; C, D, E, F, and G) cells were fixed and processed for indirect immunofluorescent microscopy after incubation at 37°C for 4 h (see MATERIALS AND METHODS). Microtubules were visualized with anti-tubulin antibodies, chromosomal DNA was visualized with DAPI, and cell shape was visualized with Nomarski. *fab1* cells with aberrant nuclear distribution and microtubule morphology are visible: aploid (large arrowheads) and binucleate (large arrows) cells, cells containing a U-shape nucleus (small arrows), unbudded mononucleate cells containing multiple spindle pole bodies (small arrowheads), an indented cell (E, F, and G, top cell), a small budded cell in which a single chromosome mass was in the bud (E, F, and G, middle cell), and a large budded cell which had a single chromosome mass located off the neck (E, F, and G, bottom cell).

content of *fab1–2* and wild-type cells was examined by flow cytometry (Yamamoto and Koshland, unpublished results). In *fab1–2* at 23°C and in wild-type cells at 23°C or 37°C, peaks of 1C and 2C DNA were observed, which corresponded to DNA content of haploid cells in G1 and G2, respectively. In contrast, 4 h after shifting the *fab1–2* culture to 37°C, cells with 1C DNA disappeared while those with more than 2C appeared. This loss of cells with G1 haploid DNA content was not the consequence of cells arresting at other stages of the cell cycle, as more than 20% of the cells in the mutant culture had the morphology of G1 cells (a single nucleus and no bud) (Table 2). Many of the G1 cells contained extra spindle pole bodies (data not shown). Taken together these results suggest that G1 cells with greater than haploid DNA content arose by the asymmetric inheritance of spindle pole bodies and chromosomes. These data support the conclusion that many *fab1* cells undergo improper chromosome segregation at 37°C.

Spindle and Nuclear Phenotypes of fab1 Mutants Are Suppressed by a Subset of vps Mutations Affecting Vacuole Morphology

Several observations suggested that the aberrant chromosome segregation observed in *fab1* cells at 37°C might be an indirect consequence of abnormal vacuole structure or function. First, in a *fab1–2* culture, the DAPI staining pattern (Table 2 and Figure 5) and the FACS profile were normal at 23°C and did not become abnormal in the majority of cells until 4 h after temperature shift to 37°C. In contrast,

vacuole morphology and acidification were partially aberrant in some *fab1–2* cells at 23°C, and became dramatically aberrant in most cells by 30 min after the temperature shift (see above). In addition, the presence of U-shaped chromosomes and bent spindles at the cell periphery correlated with the proximity of a very enlarged vacuole.

To further analyze the relationship between aberrant chromosome segregation and vacuole morphology in *fab1* mutants, we examined chromosome segregation in double mutants containing the *fab1::LEU2* insertion and various *vps* mutations. The *fab1::LEU2* mutant had phenotypes indistinguishable from the *fab1-Δ1* allele described above, i.e., abnormal vacuoles and chromosome distribution were apparent in a significant fraction of *fab1::LEU2* cells at 23°C, and this fraction increased dramatically at 37°C. The chromosome distribution in all *vps* single mutants was normal even in *vps* mutants that accumulate large vacuoles (though not as large as *fab1–2*). Double mutants harboring *fab1::LEU2* and either Δ *vps18* (class C), Δ *vps33* (class C), or *ren1/vps2* (class E) showed similar chromosome distribution to wild-type cells at 23°C and 37°C and had either no vacuoles (Δ *vps18 fab1* or Δ *vps33 fab1*) or vacuoles of reduced size (*ren1 fab1*) (Figure 6 and data not shown). In contrast, double mutants of *fab1* and Δ*vps34* (Class D) or *vps19* (Class D) had enlarged vacuoles and the *fab* phenotype was like that of the *fab1* single mutant. The fact that abnormal chromosome distribution in *fab1* mutants is eliminated by mutations in three different *vps* genes that reduce the fab vacuole morphology defect supports the hypothesis that the chromosome defect of *fab1* mutants results from the presence of an enlarged vacuole.

Cloning and Sequence Analysis of the FAB1 Gene

The *FAB1* gene was cloned by transforming *fab1–1* cells with a yeast genomic DNA library contained on a centromere-based vector (see MATERIALS AND METHODS). Ten transformants that complemented the *ts* growth of *fab1–1* were analyzed. Of these transformants, nine contained an identical plasmid with a 9-kb insert (Figure 7A, gray bar). Subclones of this insert and flanking DNA were used to map the complementing activity to a 4.8-kb *Bam*HI-*Pst*I fragment. The insert was shown to carry the authentic *FAB1* gene by linkage analysis. The *TRP1* gene was directed into the genome of a *trp1* haploid cell adjacent to the site of the insert (see MATERIALS AND METHODS). This strain was mated with a *fab1–2* strain, and the resulting diploid was sporulated. In 12 tetrads where the Fab and Trp phenotypes segregated 2:2, the Fab^+ phenotype always co-segregated with Trp^+ phenotype. These results demonstrated that this clone was derived from the *FAB1* locus. The *FAB1* clone was mapped to the right arm of chromosome VI about 40 kb from the centromere (see MATERIALS AND METHODS).

The DNA sequence of the *FAB1* locus revealed a single ORF of 6.8 kb (Figure 7A, large arrow; Figure 8). An mRNA of sufficient length to encode this ORF has been detected in the *FAB1* region of chromosome VI (Yoshikawa and Isono, 1991). However, a 4.8-kb *Bam*HI-*Pst*I fragment that lacked 2 kb from the 5′ end of this 6.8-kb ORF was capable of complementing the *fab1-Δ1* phenotypes (Figure 7, A and B). Apparently, the amino-terminal one-third of Fab1p is not needed for its function. The region of similarity between Fab1p and PIP5K maps to the 3′ end of the 6.8-kb ORF.

The amino acid sequence deduced from the 6.8-kb ORF predicted a protein of 2279 amino acids with a predicted size of 257 kDa (Figure 8A). This amino acid sequence was compared with those generated by translation of the GenBank nucleic acid data base. A 300 aa domain (between 1911 and 2233) of Fab1p exhibits 35% identity with one human protein that has been shown to have PI(4)P 5-kinase activity (Bazenet *et al.*, 1990; Boronenkov and Anderson, 1995). This region is also very similar to a region in Mss4p, a protein that was identified as a suppressor of a mutation in *STT4*, a gene that encodes one of the two known PI 4-kinases in yeast (Yoshida *et al.*, 1994a). This similarity suggests that Fab1p and Mss4p may have PI(4)P 5-kinase activity (Boronenkov and Anderson, 1995). The 300 aa region of similarity between Fab1p, Mss4p, and PIP5K-II includes a predicted nucleotide binding motif that is likely to be required for the activity of these proteins. Downstream of the nucleotide binding motif, sequences conserved among each of the proteins were identified that exhibited weak but intriguing homology to sequence motifs that are highly conserved among the family of protein kinases (Figure 8B). Mutagenesis of these conserved sequence elements will be required to address their role in the catalytic activity of these proteins.

Residues between 237 and 268 of the putative Fab1p showed significant similarity to four sequences in the data base that together appear to define a new motif (Figure 8C). The significance of this similarity was evident from the absolute conservation of the position of many rare residues, including tryptophan, cysteine, and histidine. One of the proteins with this motif, p162, appears to be an endocytic protein (accession number X78998) whereas the other, Pep7p/Vac1p/Vps19p (Jones, 1977; Weisman and Wickner, 1992), is involved in vacuole inheritance and vacuolar protein sorting. The phenotype of *fab1* mutants suggests that Fab1p may also regulate some aspect of vacuole function. Therefore, the presence of this motif in p162, Vac1p, and Fab1p may reflect some vacuole/endosome-specific function. However, because this motif is missing from *FAB1* subclones that retain complemen-

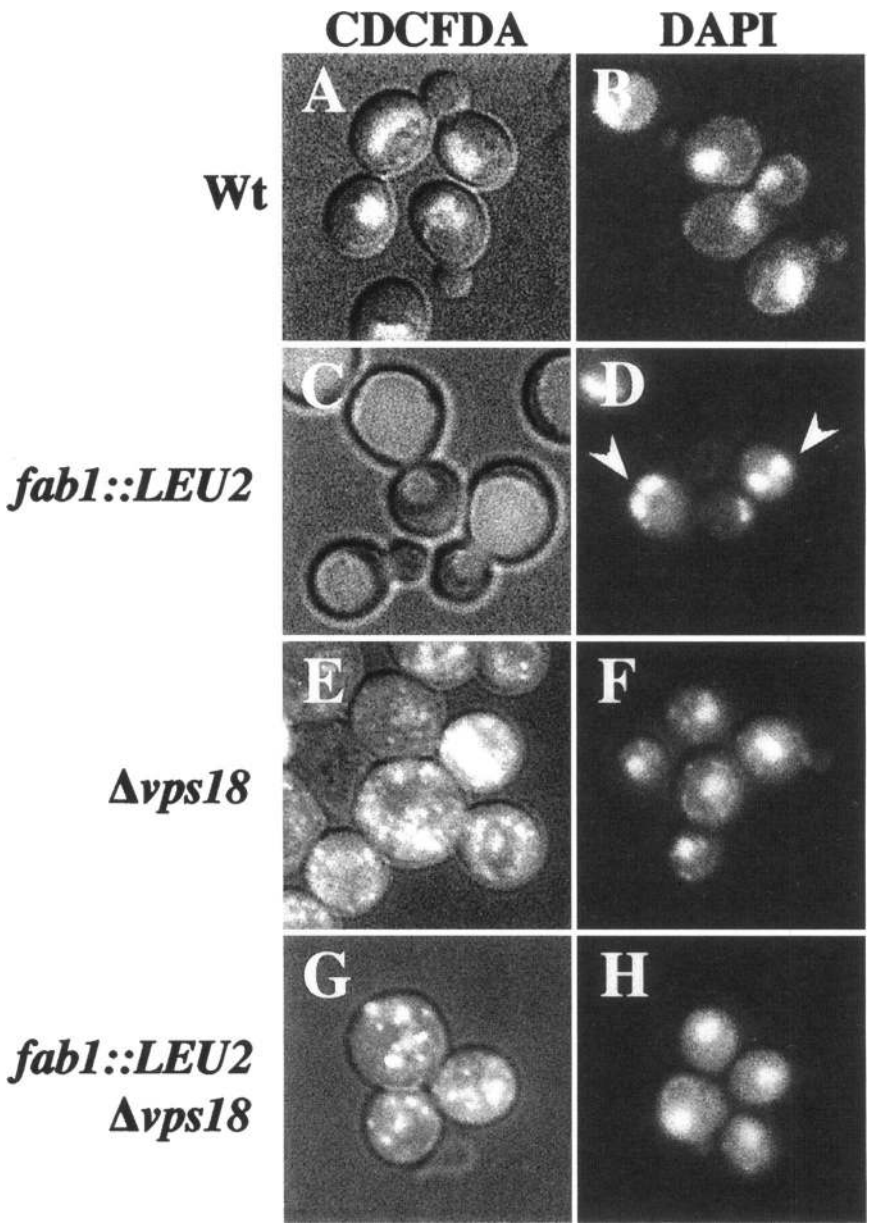

Figure 6. Vacuolar and nuclear morphology of cells with deletions of *VPS18* and *FAB1* genes. Wild-type cells (6742–1-1; A and B), *fab1*-Δ*1* cells (6742–1-3; C and D), *vps18*Δ cells (6742–1-4; E and F), and *fab1*-Δ*1 vps18*Δ cells (6742–1-2; G and H), were grown to log phase at 23°C and incubated at 37°C for 4 h. The cell cultures were split into two and were processed for vacuolar staining with CDCFDA (A, C, E, and G) and for DNA staining with DAPI (B, D, F, and H). Composite fluorescent and Nomarski images were generated. Arrowheads indicate typical binucleate cells in *fab1* mutants.

tation activity, this motif is not essential for, at least, the *FAB1* functions we assayed (cell growth, vacuole morphology, and nuclear segregation). In addition, other similarities with less obvious significance were also identified including the following: 1) a limited similarity to TCP1 proteins, 2) a motif between 1919 to 1929 that conforms to a consensus sequence (P-[SAP]-[IV]-[DN]-X-X-X-S-X-S) found in α and β subunits of vacuole ATP synthase (Senior, 1988; Futai *et al.*, 1989; Gogarten *et al.*, 1989; Nelson, 1989; Vogler *et al.*, 1991), and 3) an asparagine-rich region (from 576 to 590 residue) containing 15 contiguous asparagine residues.

DISCUSSION

In this study, we have analyzed the function of the *FAB1* gene of *S. cerevisiae* by the characterization of *fab1* mutants. The loss of Fab1p activity causes defects in the following: 1) the size and acidity of the vacuole, 2) chromosome segregation, and 3) cell surface integrity. However, the vacuole defects of *fab1* mutants are the most penetrant; a dramatic increase in vacuole size is evident in the *fab1–2 ts* mutant shortly after shift to the nonpermissive temperature, long before the appearance of chromosome missegregation and cell lysis. These results

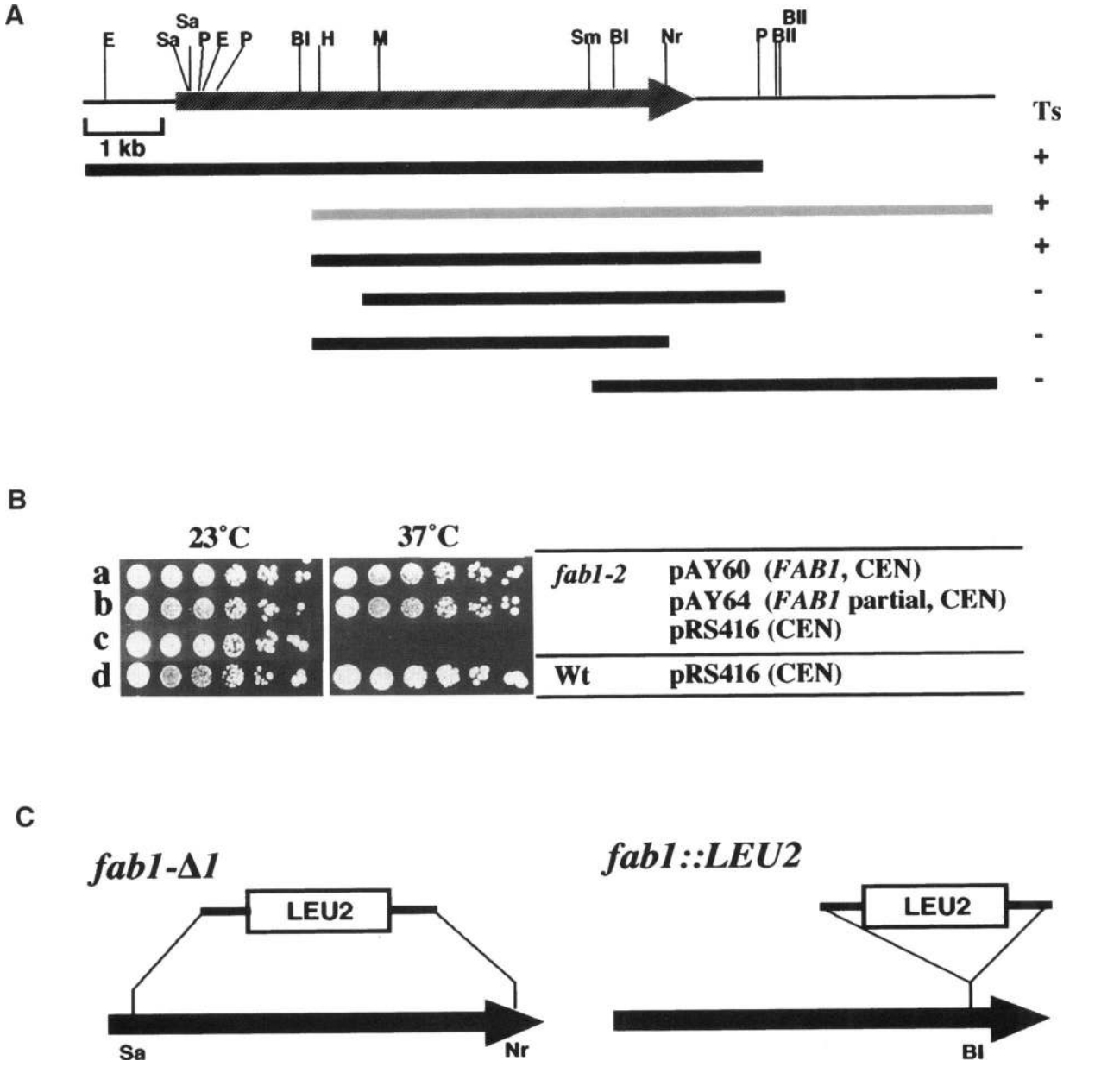

Figure 7. Cloning of *FAB1* gene. (A) Restriction analysis of region containing *FAB1* gene is shown at the top. Restriction sites are BI, *Bam*HI; BII, *Bgl*II; E, *Eco*RI; H, *Hin*dIII; K, *Kpn*I; M, *Mlu*I; P, *Pst*I; PII, *Pvu*II; Nh, *Nhe*I; Nr, *Nru*I; Sa, *Sal*I; Sm, *Sma*I; Sp, *Sph*I; and X, *Xho*I. The arrow indicates putative *FAB1* ORF. Several subclones of this region (indicated by the bars) were scored for their ability to complement (+) or not complement (−) the ts lethality of *fab1-1* (616-3-2). The gray bar indicates the insert in pAY64. (B) Qualitative comparison of the complementation of *fab1-2* by plasmids containing either the entire *FAB1* ORF (pAY60) or the minimal complementing clone (pAY64). *fab1-2* cells with the indicated plasmids were grown to log phase in selective medium at 23°C and diluted to 7×10^6 cells/ml. The cell suspensions were serially diluted by fivefold and 5 μl of each suspension was spotted on solid selective medium. The plates were incubated at 23°C or 37°C until patches were visible. As controls the same protocol was used to follow the growth of wild-type cells (c) and *fab1-2* cells with the vector pRS416 (d). (C) Two different disruptions of the *FAB1* gene. Almost the entire coding region of the *FAB1* gene was deleted by inserting a *LEU2* fragment between one of the *Sal*I sites close to the N-terminus and the *Nru*I site (*fab1-Δ1*). The C-terminal region was disrupted by inserting a *LEU2* fragment at the *Bam*HI site closer to the C-terminus (*fab1::LEU2*). These disruptions were introduced into haploids or diploids by the method of one-step gene replacement (Rothstein, 1983) and their structure was verified by Southern analysis.

suggest that the primary function of Fab1p is likely to be at the level of the vacuole. This conclusion is supported by several additional observations that associate Fap1p with the vacuole. The amino termi-

nus of Fab1p appears to contain a new motif found in other proteins implicated in vacuole or endosome function (see Figure 8C). Furthermore, preliminary localization of a Fab1p-β-galactosidase hybrid suggests that it is associated with the vacuole (Yamamoto and Koshland, unpublished results).

A significant clue to the molecular function of Fab1p comes from the observation that a 300-amino acid region of Fab1p and a human PIP5K-II share extensive similarity (Boronenkov and Anderson, 1995). PIP5K-II has been shown to be the catalytic subunit responsible for PI(4)P 5-kinase activity as its expression in *Escherichia coli* is sufficient to generate kinase activity (Boronenkov and Anderson, 1995). The region of similarity contains a nucleotide binding motif as well as other less stringent similarities to kinases (Figure 8B). These data suggest that the product of the *FAB1* gene (Fab1p) encodes a PI(4)P 5-kinase.

In support of this conclusion, the putative kinase domain of Fab1p and PIP5K-II is also found in Mss4p, another yeast protein. Indeed, Mss4p was placed in the PIP_2 metabolic pathway because its overexpression could suppress defects that resulted from lowered activity of the *STT4*-encoded PI 4-kinase (Yoshida *et al.*, 1994b). It is reasonable that lower PIP_2 levels caused by Stt4p defects could be compensated in part by elevated levels of Mss4p if Mss4p is a PI(4)P 5-kinase. The existence of at least one additional PI(4)P 5-kinase in yeast besides Fab1p is supported by the detection of significant PI(4)P 5-kinase activity in total cell extracts of *fab1*Δ strains (Anderson and Emr, unpublished data). Furthermore, precedent exists for multiple PI(4)P 5-kinases in mammalian cells (Jenkins *et al.*, 1994). PI(4)P 5-kinase activities with distinct biochemical properties have been identified in human erythrocytes (Bazenet *et al.*, 1990; Jenkins *et al.*, 1994).

The vacuole, like all other organelles, is highly dynamic with regard to the influx and efflux of membranes. The regulation of these dynamic processes is critical to the maintenance of organelle size and integrity. The extreme enlargement of the vacuole in *fab1* mutants indicates an imbalance in vacuole membrane flux and suggests that PIP_2, the putative product of Fab1p, may be critical to the regulation of vacuole membrane homeostasis. Although a defect in the processing and possibly sorting of vacuolar proteins is also observed in *fab1-Δ1* mutants (this study), this defect appears to be a secondary consequence of the loss of *fab1* function, as it appears much later than defects in vacuole pH or morphology. Furthermore, we have been unable to detect a defect in endocytosis in the *fab1–2 ts* mutant (Yamamoto and Koshland, unpublished results) or secretion (DeWald and Emr, unpublished results). These results suggest that enlargement of the vacuole in the *fab1–2* mutant does not reflect a defect in global membrane trafficking processes like endocytosis or secretion. Rather, we sug-

A

```
   1 MSSEEPHASISFPDGSHVRSSSTGTSSVNTIDATLSRPNY
  41 IKKPSLHIMSTSTTSTTTDLVTNPILSNISVPKISPPTSS
  81 SIATATSTSHVTGTASHSNIKANANTSTSVNKKNLPPTTS
 121 GRIPSSTIKRYPSRYKPSHSLQLPIKNDSNFKRSSIYASK
 161 STVTAIPIRNNRPISMQNSYARTPDSDHDDVGDEVSSIKS
 201 ASSSLTASLSKSFLFAFYNNRKKDKTSNNGVLSKEY WMKD
 241 ESSKECFSCGKTFNTFRRKHHCRICGQIFCSSCT LLIDGD
 281 RFGCHAKMRVCYNCYEHADTYEDSSDEENDSTMQLNEPRS
 321 RSRSRSSNTNPYSHSHSHLHLISQDNHNGTDLHDPVAATD
 361 NPQQQNEVYLLNDDDVQSIMTSGEDSKLFISTPPPPPKMA
 401 IPATKQGGSLEISFDSENDRALHYQDDNPGRHHHLDSVPT
 441 RYTIRDMDNISHYDTNSNSTLRPHYNTNNSTITINNLNNT
 481 TSNNSNYNNTNSNSNINNPAHSLRRSIFHYVSSNSVNKDS
 521 NNSSATPASSAQSSSILDPANRIIGNYAHRNYKFKFNYNS
 561 KGPSQQNDTANGNND NNNNNNNNNNNNNNN SASGIADNNN
 601 IPSNDNGTTFTLDKKKRNPLTKSKSTSAYLEYPLNEEDSS
 641 EDEGSMSIYSVLNDDHKTDNPIRSMRNSTKSFQRAQASLQ
 681 RMRFRRKSKSKHFPNNSKSSIYRDLNFLTNSTPNLLSVVS
 721 DDNLYDDSSPLQDKASSSAASRLTDRKFSNSSGSNNNSNS
 761 NSNINTDPWKRIASISGFKLKKEKKRELNEVSLLHMHALL
 801 KQLLNDQEISNLQEWITLLDGALRKVLRTILNARDLNTLD
 841 FRQTYVKIKRISGGSPQNSEYIDGVVFSKALPSKTMPRHL
 881 KNPRILLIMFPLEYQKNNNHFLSIESVFRQEREYLDKLVS
 921 RLKSLHPDIIYVGANVSGYALELLNDSGIVVQFNMKPQVI
 961 ERIAKLTEADIAISVDKLATNIKMGECETFEVKSYIYGNI
1001 SKTYTFLRGCNPELGGTILLRGDSLENLRKIKQVSEFMVY
1041 AIFSLKLESSFFNDNFIQLSTDVYLKRAESKKLQVFEGYF
1081 ADFLIKFNNRILTVSPTVDFPIPFLLEKARGLEKKLIERI
1121 NQYESESDLDRQTQLNMLQGLESTITKKHLGNLIKFLHEM
1161 EIENLELEFQKRSRQWEVSYSSSQNLLGTGSHQSITVLYS
1201 MVSTKTATPCVGPQIVTIDYFWDSDISIGQFIENVVGTAR
1241 YPCQQGCNGLYLDHYRSYVHGSGKVDVLIEKFQTRLPKLK
1281 DIILTWSYCKKCGTSTPILQISEKTWNHSFGKYLEVMFWS
1321 YKDSVTGIGKCPHDFTKDHVKYFGYNDLVVRLEYSDLEVH
1361 ELITPPRKIKWKPHIDIKLKVELYYKILEKINNFYGSVLS
1401 RLERIKLDSMTKDKVLSGQAKIIELKSNATEEQKLMLQDL
1441 DTFYADSPCDQHLPLNLVIKSLYDKAVNWNSTFAIFAKSY
1481 LPSETDISRITAKQLKKLFYDSSRKDSEDKKSLHDEKAKT
1521 RKPEKNELPLEGLKDVEKPKIDSKNTTENRDRTNEPQNAV
1561 TITTFKDDTPIIPTSGTSHLTVTPSASSVSSSLTPQTEER
1601 PPISRSGTGISMTHDKSTRPNIRKMSSDSSLCGLASLANE
1641 YSKNNKVSKLATFFDQMHFDALSKEFELERERERLQLNKD
1681 KYQAIRLQTSTPIVEIYKNVKDAVDEPLHSRSSGNNLSSA
1721 NVKTLEAPVGEHSRANNCNPPNLDQNLETELENSISQWGE
1761 NILNPSGKTTASTHLNSKPVVKETSENPKSIVRESDNSKS
1801 EPLPPVITTTTVNKVESTPQPEKSLLMKTLSNFWADRSAY
1841 LWKPLVYPTCPSEHIFTDSDVIIREDEPSSLIAFCLSTSD
1881 YRNKMMNLNVQQQQQQQTAEAAPAKTGGNSGGTTQTGDPS
1921 VNISPSVSTTSHNKGRDSEISSLVTTKEGLLNTPPIEGAR
1961 DRTPQESQTHSQANLDTLQELEKIMTKKTATHLRYQFEEG
2001 LTVMSCKIFFTEHFDVFRKICDCQENFIQSLSRCVKWDSN
2041 GGKSGSGFLKTLDDRFIIKELSHAELEAFIKFAPSYFEYM
2081 AQAMFHDLPTTLAKVFGFYQIQVKSSISSSKSYKMDVIIM
2121 ENLFYEKKTTRIFDLKGSMRNRHVEQTGKANEVLLDENMV
2161 EYIYESPIHVREYDKKLLRASVWNDTLFLAKMNVMDYSLV
2201 IGIDNEGYTLTVGIIDFIRTFTWDKKLESWVKEKGLVGGA
2241 SVIKQPTVVTPRQYKKRFREAMERYILMVPDPWYREGNZ
```

Figure 8. (A) Amino acid sequence of Fab1p, predicted from the nucleotide sequence of the putative *FAB1* ORF, is shown by single letters. The nucleotide sequence is available under the GenBank accession number U01017. A stretch of 15 asparagine amino acids is

gest that the enlargement of the vacuole occurs because Fab1p is required for the efficient efflux/turnover of vacuole membrane.

The idea that PIP_2 might be an important regulator of vacuole membrane homeostasis may reflect a more general role of PIP_2 as a regulator of membrane trafficking events. Interestingly, other mutants with defects in PI metabolism have been identified that alter membrane trafficking events. Sec14p, a PI/PC transfer protein, is required for secretion by maintaining the proper lipid content of the Golgi (Cleves *et al.*, 1991). Vps34p, a PI 3-kinase, is required for proper sorting of proteins to the vacuole (Herman and Emr, 1990; Schu *et al.*, 1993). Finally the cell lysis defects associated with other PIP_2 metabolic enzymes may reflect an imbalance of plasma membrane flux and cell wall synthesis.

If Fab1p function is restricted primarily to the vacuole, why do *fab1* mutants show defects in cell surface integrity, spindle orientation, and nuclear division? One explanation for these secondary defects is that the extreme size of the vacuoles in *fab1* mutants sterically interferes with cell surface and nuclear processes. This model is supported by the observation that the spindle misorientation and nuclear division defects of *fab1* mutants are eliminated when vacuole size is reduced by specific *vps* mutations.

Another explanation for the secondary defects exhibited by *fab1* mutants is that PIP_2 regulates cell surface and nuclear functions as well as vacuole functions, perhaps by compartmentalization of PIP_2 metabolic isozymes to each of these organelles. The blockage of the vacuole PIP_2 pathway by *fab1* mutations may generate aberrant signals that eventually interfere with the nuclear and/or cell surface PIP_2 pathways, hence the secondary defects. The existence of PIP_2 metabolic pathways dedicated to cell surface and nuclear processes is supported by the observation that mutations in other PIP_2 metabolic enzymes cause primary defects in cell lysis, recombination, and chromosome segregation but not vacuoles (Levin and Bartlett-Heubusch, 1992; Flanagan *et al.*, 1993; Flick and Thorner, 1993; Payne and Fitzgerald-Hayes, 1993; Nuange and Symington, 1994; Yoshida *et al.*, 1994a). Furthermore, at least one of these enzymes (Pik1p) has been localized to the nucleus (Garciabustos *et al.*, 1994).

The model of multiple sites for PIP_2 metabolism predicts that several isozymes of PI(4)P 5-kinase may exist that have different functions depending upon their site of action. In fact, *MSS4*, the other gene encoding a putative PI(4)P 5-kinase, is essential for viability unlike *FAB1* (Yoshida *et al.*, 1994b). Furthermore, Fab1p and Mss4p share no similarity outside of the kinase domain (this study). These results are consistent with the idea that Mss4p and Fab1p have distinct biological roles, perhaps by acting at different sites. As the *MSS4* gene was identified as a high copy suppressor of a *stt4* mutation (Yoshida *et al.*, 1994b), it is possible that Mss4p and Stt4p may function at the same site. The products of the *TOR1* and *TOR2* genes share homology with PI 3- or PI 4-kinases and are likely also to be PI kinases. Interestingly, when galactose-regulated Tor2p expression is turned off in a *tor1/tor2* double mutant background, cells acquire very enlarged vacuoles similar to those observed in *fab1* mutants (Kunz *et al.*, 1993). Based upon this phenotypic similarity, it is possible that Tor2p may act at the same site as Fab1p. The construction and phenotypic characterization of *fab1 mss4* and *fab1 tor2* mutants

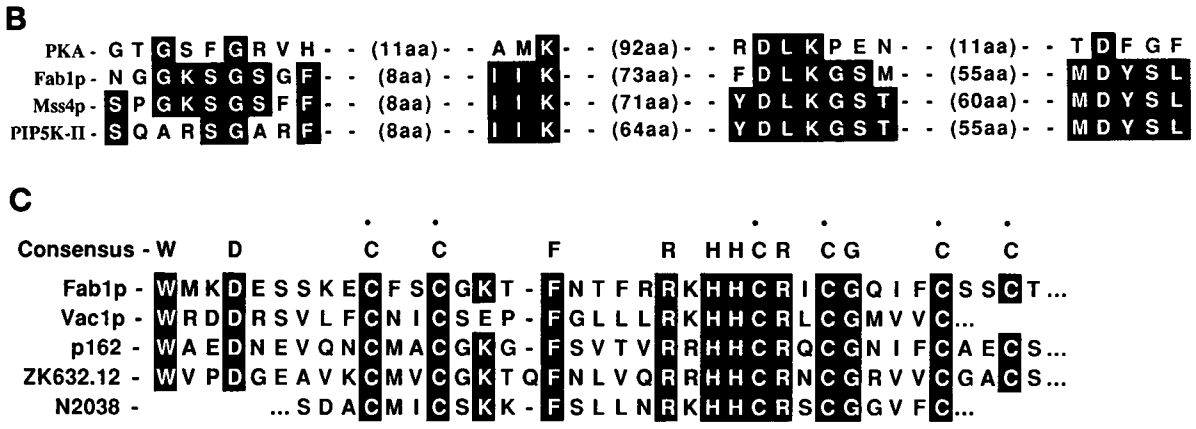

Figure 8 cont. indicated in bold. (B) Sequence identities are shown between a subset of highly conserved motifs found in protein kinases (Hanks *et al.*, 1988) [like the cAMP dependent protein kinases (PKA)] and highly conserved regions of Fab1p, Mss4p, and PIP5K-II. (C) Alignment showing similarity of residues of putative Fab1p to Vac1p, p162, and several partial ORF's from *Caenorthabditis elegans* (ZK632.12) and *S. cerevisiae* (N2038). The zinc-finger–like domain was highlighted with dots. Accession numbers of p162, ZK632.12, and N2038 are X78998, Z22181, and X77395, respectively.

should help to elucidate the functional interactions between Fab1p, Mss4p, and Tor2p.

In conclusion the complex phenotype of *fab1* mutants suggest that the synthesis of PIP_2 is an important metabolite for the function and morphology of the vacuole as well as cell surface and nuclear processes. Unraveling the specific biological function of Fab1p will require additional characterization of its cellular location, its precise biochemical activity, and the identification of the specific targets of its product, "PIP_2".

ACKNOWLEDGMENTS

We thank Forest Spencer for giving us the DNA library, Seiji Tanaka and Katsumi Isono for giving us a λ phage clone I-1B12, and Nick Davis for giving us the *ren1* strain. We thank Jim Flook for operating the flow cytometer and generating profiles of the pH of vacuoles and MaryLynne LaMantia for her assistance in the initial characterization of the vacuole defects in *fab1* mutants. We thank Kathleen Wilsbach, Jeff Stack, and others for critical reading of the manuscript and Christine Norman for assisting in manuscript preparation. This work was supported by grants from the National Institutes of Health (GM-41718, D.E.K. and A.Y.; GM-51968 and GM-38906, R.A.A.) and a grant from the National Cancer Institute (CA-58689, S.D.E.). S.D.E. is supported as an Investigator of the Howard Hughes Medical Institute. A.Y. is the recipient of a Fellowship of the Naito Foundation. D.B.D. is the recipient of a National Science Foundation Plant Biology Postdoctoral Fellowship (BIR-9303758).

REFERENCES

Bazenet, C.E., Ruano, A.R., Brockman, J.L., and Anderson, R.A. (1990). The human erythrocyte contains two forms of phosphatidylinositol 4-phosphate 5-kinase which are differentially active toward membranes. J. Biol. Chem. *265*, 18012-18022.

Berridge, M.J., and Irvine, R.F. (1989). Inositol phosphates and cell signaling. Nature *341*, 197–205.

Boronenkov, I.V., and Anderson, R.A. (1995). Phosphatidylinositol 4-phosphate 5-kinase is a novel lipid kinase with yeast homologues. J. Biol. Chem. *270*, 2881–2884.

Buxeda, R.J., Nickels, J.T., Belunis, C.J., and Carman, G.M. (1991). Phosphatidylinositol 4-kinase from *Saccharomyces cerevisiae*. J. Biol. Chem. *266*, 13859-13865.

Carpenter, C.L., and Cantley, L.C. (1990). Phosphoinositide kinases. Biochemistry *29*, 11147-11156.

Cleves, A., McGee, T., and Bankaitis, V. (1991). Phospholipid transfer proteins: a biological debut. Trends Cell Biol. *1*, 30–34.

Flanagan, C.A., Schnieders, E.A., Emereick, A.W., Kunisawa, R., Admon, A., and Thorner, J. (1993). Phosphatidylinositol 4-kinase: gene structure and requirement for yeast cell viability. Science *262*, 1444–1448.

Flanagan, C.A., and Thorner, J. (1992). Purification and characterization of a soluble phosphatidylinositol 4-kinase from the yeast *Saccharomyces cerevisiae*. J. Biol. Chem. *267*, 24117-24125.

Flick, J.S., and Thorner, J. (1993). Genetic and biochemical characterization of a phosphatidylinositol-specific phospholipase C in *Saccharomyces cerevisiae*. Mol. Cell. Biol. *13*, 5861–5876.

Futai, M., Noumi, T., and Maeda, M. (1989). ATP synthase (H^+-ATPase): results by combined biochemical and molecular biological approaches. Ann. Rev. Biochem. *58*, 111–136.

Garciabustos, J.F., Marini, F., Stevenson, I., Frei, C., and Hall, M.N. (1994). PIK1, an essential phosphatidylinositol 4-kinase associated with the yeast nucleus. EMBO J. *13*, 2352–2361.

Gogarten, J.P., Kibak, H., Dittrich, P., Taiz, L., Bowman, E.J., Bowman, B.J., Manolson, M.F., Poole, R.J., Date, T., Oshima, T., Konishi, J., Denda, K., and Yoshida, M. (1989). Evolution of the vascular H^+-ATPasse; implications for the origin of eukaryotes. Proc. Natl. Acad. Sci. USA *86*, 6661–6665.

Hanks, S.K., Quinn, A.M., and Hunter, T. (1988). The protein kinase family: conserved features and deduced phylogeny of the catalytic domains. Science *241*, 42–52.

Herman, P.K., and Emr, S.D. (1990). Characterization of *VPS34*, a gene required for vacuolar protein sorting and vacuole segregation in *Saccharomyces cerevisiae*. Mol. Cell. Biol. *10*, 6742–6754.

Herman, P.K., Stack, J.H., and Emr, S.D. (1992). An essential role for a protein and lipid kinase complex in secretory protein sorting. Trends Cell Biol. *2*, 363–368.

Hutter, K.J., and Eipel, H.E. (1978). Flow cytometric determinations of cellular substances in algae, bacteria, molds and yeast. Antonie van Leeuwenhoek *44*, 269–282.

Ito, H., Fukuda, Y., Murata, K., and Kimura, A. (1983). Transformation of intact yeast cells treated with alkali cations. J. Bacteriol. *153*, 163–168.

Janmey, P. (1994). Phosphoinositides and calcium as regulators of cellular actin assembly and disassembly. Annu. Rev. Physiol. *56*, 169–191.

Janmey, P., and Stossel, T. (1989). Gelsolin-polyphosphoinositide interaction. J. Biol. Chem. *264*, 4825–4831.

Jenkins, G.H., Fissette, P.L., and Anderson, R.A. (1994). Type I phosphatidylinositol 4-phosphate 5-kinase isoforms are specifically stimulated by phosphatidic acid. J. Biol. Chem. *269*, 11547-11554.

Jones, E.W. (1977). Proteinase mutants of *Sacchromyces cerevisiae*. Genetics *85*, 23–33.

Kapeller, R., and Cantley, L.C. (1994). Phosphatidylinositol 3-kinase. BioEssays *16*, 565–576.

Kilmartin, J., and Adams, A. (1984). Structural rearrangements of tubulin and actin during the cell cycle of the yeast *Saccharomyces*. J. Cell Biol. *98*, 922–933.

Kilmartin, J.V., Wright, B., and Milstein, C. (1982). Rat monoclonal antitubulin antibodies derived by using a new nonsecreting rat cell line. J. Cell. Biol. *93*, 576–582.

Klionsky, D.J., Herman, P.K., and Emr, S.D. (1990). The fungal vacuole: composition, function, and biogenesis. Microbiol. Rev. *54*, 266–292.

Kunz, J., Henriquez, R., Schneider, U., Deuter-Reinhard, M., Movva, N.R., and Hall, M.N. (1993). Target of rapamycin in yeast, TOR2, is an essential phosphatidylinositol kinase homolog required for G_1 progression. Cell *73*, 585–596.

Lassing, I., and Lindberg, U. (1988). Specificity of the interaction between phosphatidylinositol 4,5-bisphosphate and the profilin:actin complex. J. Cell. Biol. *37*, 255–267.

Levin, D.E., and Bartlett-Heubusch, E. (1992). Mutants in the *S. cerevisiae PKC1* gene display a cell cycle-specific osmotic stability defect. J. Cell Biol. *116*, 1221–1229.

Ling, L.E., Schulz, J.T., and Cantley, L.C. (1990). Characterization and purification of membrane-associated phosphatidylinositol-4-phosphate kinase from human red blood cells. J. Biol. Chem. *264*, 5080–5088.

Liscovitch, M., Chalifa, V., Pertile, P., C-Chen, S., and Cantley, L.C. (1994). Novel functions of phosphatidylinositol 4,5-bisphosphate as

a cofactor for brain membrane phospholipase D. J. Biol. Chem. *269*, 21403-21406.

Nelson, N. (1989). Structure, molecular genetics, and evolution of vacuolar H^+-ATPases. J. Bioenerg. Biomembr. *21*, 553–571.

Nuange, K.N., and Symington, L.S. (1994). Mutation of the gene encoding protein kinase C1 stimulates mitotic recombination in *Saccharomyces cerevisiae*. Mol. Cell. Biol. *14*, 6039–6045.

Palmer, R., Hogan, E., and Koshland, D. (1990). Mitotic transmission of artificial chromosomes in *cdc* mutants of the yeast, *Saccharomyces cerevisiae*. Genetics *125*, 763–774.

Payne, W.E., and Fitzgerald-Hayes, M. (1993). A mutation in *PLC1*, a candidate phosphoinositide-specific phospholipase C gene from *Saccharomyces cerevisiae*, causes aberrant mitotic chromosome segregation. Mol. Cell. Biol. *13*, 4351–4364.

Preston, R.A., Reinagel, P.S., and Jones, E.W. (1992). Genes required for vacuolar acidity in *Saccharomyces cerevisiae*. Genetics *131*, 551–558.

Roberts, C.J., Raymond, C.J., Yamashiro, C.T., and Stevens, T.H. (1991). Methods for studying the yeast vacuole. In: Guide to Yeast Genetics and Molecular Biology, ed. C. Guthrie and G.R. Fink, San Diego, CA: Academic Press, 644–661.

Rose, M.D., Winston, F., and Hieter, P. (1990). Methods in Yeast Genetics, A Laboratory Course Manual. Cold Spring Harbor, NY: Cold Spring Harbor Laboratory Press.

Rothstein, R.J. (1983). One-step gene disruption in yeast. Methods Enzymol. *101*, 202–211.

Schu, P.V., Takegawa, K., Fry, M.J., Stack, J.H., Waterfield, M.D., and Emr, S.D. (1993). Phosphatidylinositol 3-kinase encoded by yeast *VPS34* gene essential for protein sorting. Science *260*, 88–91.

Senior, A.E. (1988). ATP synthesis by oxidative phosphorylation. Physiol. Rev. *68*, 177–231.

Sullivan, D., and Huffaker, T. (1992). Astral microtubules are not required for anaphase B in *Saccharomyces cerevisiae*. J. Cell Biol. *119*, 379–388.

Vogler, A.P., Homma, M., Irikura, V.M., and Macnab, R.M. (1991). *Salmonella typhimurium* mutants defective in flagellar filament regrowth and sequence similarity of Fli1 to F_OF_1, vacuolar, and archaebacterial ATPase subunits. J. Bacteriol. *173*, 3564–3572.

Weisman, L.S., and Wickner, W. (1992). Molecular characterization of *VAC1*, a gene required for vacuole inheritance and vacuole protein sorting. J. Biol. Chem. *267*, 516–623.

Yoshida, S., Ohya, Y., Goebl, M., Nakano, A., and Anraku, Y. (1994a). A novel gene, *STT4*, encodes a phosphatidylinositol 4-kinase in the PKC1 protein kinase pathway of *Saccharomyces cerevisiae*. J. Biol. Chem. *269*, 1166–1171.

Yoshida, S., Ohya, Y., Nakano, A., and Anraku, Y. (1994b). Genetic interactions among genes involved in the *STT4-PKC1* pathway of *Saccharomyces cerevisiae*. Mol. Gen. Genet. *242*, 631–640.

Yoshikawa, A., and Isono, K. (1991). Construction of an ordered clone bank and systematic analysis of the whole transcripts of chromosome VI of *Saccharomyces cerevisiae*. Nucleic Acids Res. *19*, 1189–1195.